CMS Draft Analysis Note

2011/06/15
Head Id: 61232
Archive Id: 19233:61233M
Archive Date: 2011/06/15
Archive Tag: trunk

Search for Supersymmetry in all-hadronic events with α_T

R. Bainbridge[1], B. Betchart[2], O. Buchmüller[1], D. Burton[1], H. Flächer[2], Z. Hatherell[1], E. Laird[3], B. Mathias[1], P. Sphicas[4], and M. Stoye[4]

[1] Imperial College, London, UK
[2] University of Rochester, Rochester, NY, USA
[3] Princeton University, Princeton, NJ, USA
[4] CERN, Geneva, Switzerland

Abstract

We present an update of the search for supersymmetry in events with jets and missing transverse energy as presented in Ref. [1]. The results are based on a data sample of 350 pb^{-}1 of integrated luminosity recorded at $\sqrt{s}$ = 7 TeV. In this search, the variable α_T is used as the main discriminator between events with real and fake missing transverse energy and no excess of events over the Standard Model expectation is found. Given this agreement, exclusion limits in the parameter space of the constrained minimal supersymmetric model are set. Squark and gluino masses of 1 TeV can be excluded for values of the common scalar mass at the GUT scale $m_0 < 420$ GeV.

Contents

1 Introduction

In this note we present an update of the search for a missing energy signature in dijet and multijet events using the α_T variable. The current results are based on 350 pb^{-1} of LHC data recorded in 2011 at a centre-of-mass energy of $\sqrt{s} = 7$ TeV.

The presented search concentrates on event topologies in which heavy new particles are pair-produced in a proton-proton collision and where at the end of their decay chain a weakly interacting massive particle (WIMP) is produced. The latter remains undetected, thus leading to a missing energy signature. In the case of SUSY, squarks and gluinos could be the heavy particles while the lightest (and stable) neutralino χ_1^0 is the WIMP candidate. Although this search will be carried out in the context of SUSY, it is applicable to other New Physics scenarios as the missing energy signature is common to many models, e.g., Extra Dimensions and Little Higgs models.

Events with n high-p_T hadronic jets are studied and missing transverse momentum is inferred through the measured jet momenta via the kinematic variable α_T. The analysis follows closely Ref. [1] and two previous PAS documents [2, 3]. The variable α_T was initially inspired by Ref. [4]. The main difference with respect to Ref. [1] is that rather than defining a specific signal region, we now search for an excess of events in data over the Standard Model expectation over the entire $H_T = \sum_{i=1}^{N_{jet}} {E_T}^{j_i}$ range above 275 GeV.

The by far dominant background from multi-jet QCD events can be suppressed effectively with the α_T variable. To estimate the remaining backgrounds we make use of data control samples. These are a μ + jets sample for the background from W + jets and $t\bar{t}$ events and a photon+jets sample to determine the background from $Z \to \nu\bar{\nu}$ events.

This note is organized as follows: In Section 2 the used data and Monte Carlo (MC) samples are listed. The event selection and analysis method is described in Section 4, followed by a discussion of the data-driven methods that were developed for background estimation. Systematic uncertainties on the signal efficiency are discussed in Section 5. The statistical method used for the interpretation of the results is discussed in Section 6 and limits in the CMSSM parameter space are presented in Section 7 before concluding.

2 Data and Monte Carlo Samples

This section list the data samples and triggers that were used for the analysis. The results presented in this note are based on the following data samples:

```
/HT/Run2011A-May10ReReco-v1/AOD
/HT/Run2011A-PromptReco-v4/AOD
```

The sum of data from these samples corresponds to an integrated luminosity $353 pb^{-1}$certified in the official JSON from June 10th 2011.

For the $W \to \mu\ \nu$ sample, the following data samples are used:

```
/MuHad/Run2011A-May10ReReco-v1/AOD
/MuHad/Run2011A-PromptReco-v4/AOD
```

The sum of data from these samples corresponds to an integrated luminosity $361 pb^{-1}$certified in the official JSON from June 10th 2011.

For the photon control sample, the following datasets are used:

```
/Photon/Run2011A-May10ReReco-v1/AOD
/Photon/Run2011A-PromptReco-v4/AOD
```

The sum of data from these samples corresponds to an integrated luminosity $469 pb^{-1}$certified in the official JSON from June 10th 2011.

The signal and background Monte Carlo samples for this analysis are taken from a mixture of Fall10 and Spring11 simulation production for physics at 7 TeV

```
/QCD_Pt_*_TuneZ2_7TeV_pythia6/Spring11-PU_S1_START311_V1G1-v1/AODSIM
/QCD_TuneD6T_HT-*_7TeV-madgraph/Spring11-PU_S1_START311_V1G1-v1/AODSIM
/TTJets_TuneZ2_7TeV-madgraph-tauola/Spring11-PU_S1_START311_V1G1-v1/AODSIM
/TToBLNu_TuneZ2_*-channel_7TeV-madgraph/Spring11-PU_S1_START311_V1G1-v1/AODSIM
/WJetsToLNu_TuneZ2_7TeV-madgraph-tauola/Spring11-PU_S1_START311_V1G1-v1/AODSIM
/ZinvisibleJets_7TeV-madgraph/Spring11-PU_S1_START311_V1G1-v1/GEN-SIM-RECO
/GJets_TuneD6T_HT-40To100_7TeV-madgraph/Spring11-PU_S1_START311_V1G1-v1/AODSIM
/LM*_SUSY_sftsht_7TeV-pythia6/Spring11-PU_S1_START311_V1G1-v1/AODSIM
```

3 Triggers

The trigger strategy has changed from that of the 2010 analysis, where a pure H_T trigger was used to collect both the signal and the control samples. With the increase in instantaneous luminosity seen in 2011, these pure H_T triggers have too high thresholds for the analysis. We now move to a cross object triggers between H_T and $\not{H}_T$ for the hadronic signal region, a suite of prescaled pure H_T triggers for the hadronic control regions, H_T crossed with a muon for the muon control sample and a single object photon trigger for the photon control sample. Another major change from the 2010 analysis is that the HLT has moved to using corrected jets to calculate HT. This greatly improves the turn ons with regards to offline Calo H_T. To make sure we are fully efficient the offline bin edges have been shifted up by 25 GeV with respect to the online values.

3.0.1 Fully Hadronic Triggers

The hadronic object cross trigger lowers the accepted rate by requiring H_T and $\not{H}_T$. During the course of the analysis the thresholds have evolved with the scaling of instantaneous luminosity. The trigger paths used to collect the hadronic sample are: `HLT_HT260_MHT60_v*, HLT_HT250_MHT60_v*` `HLT_HT250_MHT60_v*, HLT_HT250_MHT70_v*, HLT_HT250_MHT80_v*`

3.0.2 Muon Control Region Triggers

The muon control sample uses a cross object trigger which requires the presence of a muon and H_T in the event. This gives access to lower p_T muons than are available from the single object muon triggers. The trigger selection used to collect this sample is the lowest unprescaled at any time from: `HLT_Mu5_HT200, HLT_Mu8_HT200, HLT_Mu15_HT200, HLT_Mu20_HT200`

3.0.3 Photon Triggers

Due to the offline requirement of a high p_T photon, the use of a single object trigger is still possible. The triggers used to collect the photon control sample are `HLT_Photon75_CaloIdVL`,

HLT_Photon75_CaloIdVL_IsoL,HLT_Photon90_CaloIdVL,HLT_Photon90_CaloIdVL_IsoL.

4 Event Selection and Analysis

The analysis follows closely Ref. [1] and is described in detail in Ref. [5]. Events with two or more high-p_T jets are selected. Specifically, jets are reconstructed using the anti-k$_T$ algorithm [6] with a size parameter of 0.5 and are required to have $E_T > 50\,\text{GeV}$, $|\eta| < 3$ and to pass jet identification criteria [7] designed to reject spurious signals in the calorimeters. The pseudorapidity of the jet with the highest E_T (leading jet) is required to be within $|\eta| < 2.5$ and the transverse energy of each of the two leading jets must exceed 100 GeV.

Events with jets passing the E_T threshold but not satisfying the jet identification criteria or the η acceptance requirement are vetoed, as this deposited energy is not accounted for in the event kinematics. Similarly, events in which an isolated lepton (electron [8] or muon [9]) with $p_T > 10\,\text{GeV}$ is identified are rejected to suppress events with genuine missing energy from neutrinos. Furthermore, to select a pure multi-jet topology, events are vetoed in which an isolated photon [10] with $p_T > 25\,\text{GeV}$ is found.

Events are required to fulfill $H_T = \sum_{i=1}^{N_{jet}} {E_T}^{j_i} > 275\,\text{GeV}$. As the main discriminator against QCD multijet production the variable α_T, defined as:

$$\alpha_T = {E_T}^{j_2} / M_T = \frac{{E_T}^{j_2}}{\sqrt{\left(\sum_{i=1}^{2} {E_T}^{j_i}\right)^2 - \left(\sum_{i=1}^{2} p_x^{j_i}\right)^2 - \left(\sum_{i=1}^{2} p_y^{j_i}\right)^2}},$$

is used and events are required to have $\alpha_T > 0.55$.

To protect against multiple jets failing the $E_T > 50\,\text{GeV}$ selection requirement, the jet-based estimate of the missing energy, $\not{H}_T$, is compared to the calorimeter tower-based estimate, ${\not{E}_T}^{calo}$, and events with $R_{miss} = \not{H}_T / {\not{E}_T}^{calo} > 1.25$ are rejected.

Finally, to protect against severe energy losses, events with significant jet mismeasurements caused by masked regions in the ECAL (which amount to about 1% of the ECAL channel count) or by missing instrumentation in the barrel-endcap gap are removed with the following procedure. The jet-based estimate of the missing transverse energy, $\not{H}_T = |\vec{\not{H}}_T| = |-\sum_{jets} \vec{p}_{T_{jet}}|$, is used to identify jets most likely to have given rise to the $\not{H}_T$ as those whose momentum is closest in ϕ to the total $\vec{\not{H}}_T$ which results after removing them from the event. The azimuthal distance between this jet and the recomputed $\not{H}_T$ is referred to as $\Delta\phi^*$ in what follows. Events with $\Delta\phi^* < 0.5$ are rejected if the distance in the (η, ϕ) plane between the selected jet and the closest masked ECAL region, ΔR_{ECAL}, is smaller than 0.3. Similarly, events are rejected if the jet points within 0.3 in η of the ECAL barrel-endcap gap at $|\eta| = 1.5$.

For reasons of simplicity and robustness the 2010 analysis used a cut-and-count approach to search for an excess of events over the SM expectation. In order to gain additional sensitivity to higher-mass states it is possible to make an interpretation of the observed and expected number of events by splitting the original signal region into multiple H_T bins. Therefore, the simple cut-and-count interpretation of one signal bin becomes a H_T shape analysis based on several bins. This requires that the data driven background methods used to determine the expected number of SM background events in the signal region provide an estimate for each of the H_T bins in the signal region of $H_T > 275\,\text{GeV}$. The data driven background methods used for the RA1 analysis were explicitly designed with this use-case in mind. In the following,

the results for the different background prediction methods are presented when splitting the signal region into 8 bins, as defined in Table 1, which is the optimal number of bins that can be exploited for the current data set.

The results of this selection are documented in Table 1 and Data and Monte Carlo comparisons for control variables are show in Section 4.1

Table 1: Definition of the H_T bins and the corresponding p_T thresholds for the leading, second and all remaining jets in the event; the number of events passing and failing the α_T cut and the resulting R_{α_T} value, for 353 pb^{-1} of data collected in 2011.

H_T Bin (GeV)	275–325	325–375	375–475	475–575
$p_T^{leading}$ (GeV)	73.3	86.7	100.0	100.0
p_T^{second} (GeV)	73.3	86.7	100.0	100.0
p_T^{other}(GeV)	36.7	43.3	50.0	50.0
$\alpha_T > 0.55$	254	118	66	19
$\alpha_T < 0.55$	1.92e+07	7.87e+06	5.39e+06	1.70e+06
R_{α_T}	1.32e-05 $\pm$ 8.31e-07$_{stat}$	1.50e-05 $\pm$ 1.38e-06$_{stat}$	1.22e-05 $\pm$ 1.51e-06$_{stat}$	1.12e-05 $\pm$ 2.56e-06$_{stat}$
H_T Bin (GeV)	575–675	675–775	775–875	875–∞
$p_T^{leading}$ (GeV)	100.0	100.0	100.0	100.0
p_T^{second} (GeV)	100.0	100.0	100.0	100.0
p_T^{other} (GeV)	50.0	50.0	50.0	50.0
$\alpha_T > 0.55$	11	1	2	1
$\alpha_T < 0.55$	5.90e+05	2.28e+05	9.61e+04	8.60e+04
R_{α_T}	1.87e-05 $\pm$ 5.62e-06$_{stat}$	4.39e-06 $\pm$ 5.04e-06$_{stat}$	2.08e-05 $\pm$ 1.47e-05$_{stat}$	1.16e-05 $\pm$ 1.34e-05$_{stat}$

4.1 Data to Monte Carlo comaprison for control variables

The following we show data-MC comparisons before the α_T cut. Theses are shown to give a general impression of the quality of the simulation. The actual background yields are obtained from data control samples as described further below.

Figures 1a & 1b show the comparisons between Data and Monte Carlo for H_T and the number of jets observed per event before an α_T cut, a high level of agreement is observed between Data and Monte Carlo.

Figures 1c & 1d show the QCD rejection power of the α_T variable, the number of QCD events falls to zero after a cut of $\alpha_T > 0.55$.

Figures 2a, 2b& 2c show comparisons between simulated standard model distributions and data for events passing the α_T selection cut. The observed distributions in data show no deviation from the standard model prediction.

4.2 H_T dependence of R_{α_T}

The ratio $R_{\alpha_T} = N^{\alpha_T > \theta}/N^{\alpha_T < \theta}$ exhibits no dependence on H_T if θ if chosen such that the numerator of the ratio in all H_T bins is dominated by EWK events and there is no significant contribution from QCD [1]. This has been demonstrated using MC simulations for the cut value $\theta = 0.55$ over the range $275 < H_T < 875$ (beyond which the available statistics are not sufficient).

One important ingredient in the R_{α_T} method is the scaling of the jet p_T thresholds in the low H_T bins to maintain jet multiplicities and thus comparable event kinematics and topologies in the different H_T bins. This is especially important in the case of the $t\bar{t}$ background, in which higher

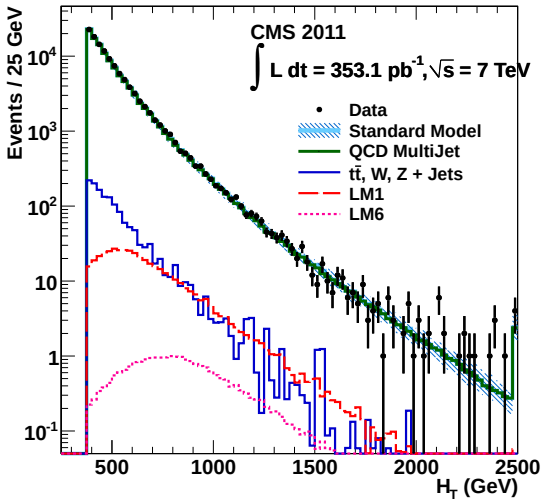

(a) Comparison of H_T between Data and Monte Carlo for the hadronic selection in the region $H_T \geq 375$ GeV.

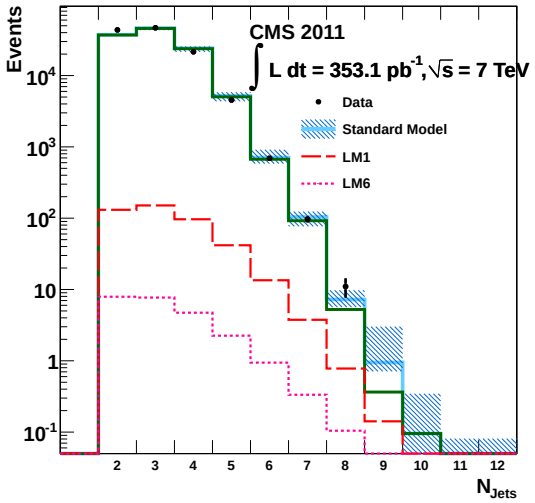

(b) Comparison of the N Jet distribution between Data and Monte Carlo for the hadronic selection, in the region $H_T \geq 375$ GeV.

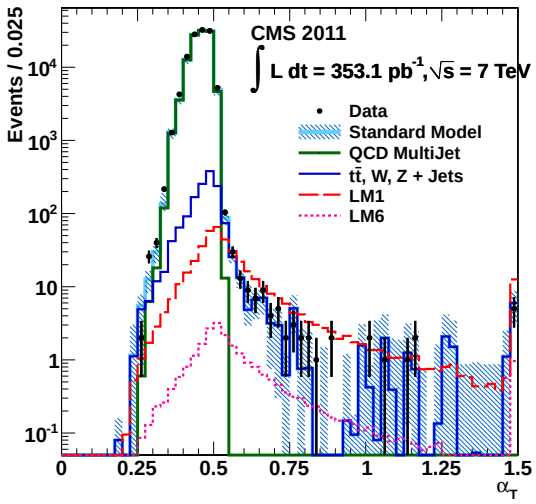

(c) Comparison of the α_T distribution between Data and Monte Carlo for the hadronic selection, in the region $H_T \geq 375$ GeV.

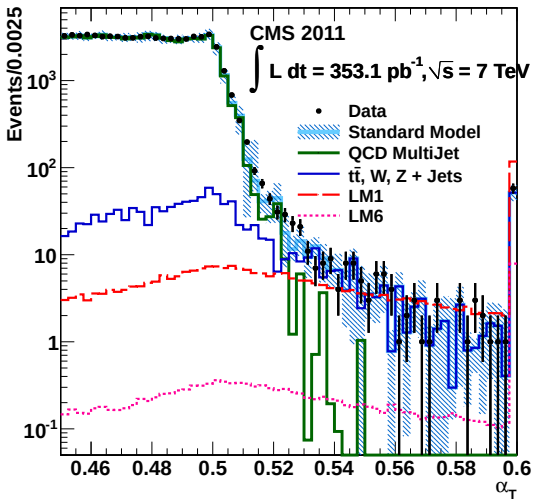

(d) Comparison of the α_T distribution highlighting the agreement on the sharply falling edge between Data and Monte Carlo for the hadronic selection, in the region $H_T \geq 375$ GeV.

Figure 1: Comparisons of basic quantities before the α_T selection cuts.

jet multiplicities can be expected relative to the other EWK backgrounds. Thus, its contribution to R_{α_T} is suppressed in the lowest H_T bins, unless the jet p_T thresholds are scaled down with the H_T lower bin boundaries. This effect is less pronounced when beyond the turn-on of the $t\bar{t}$ H_T distribution and in the exponential tail. Thus, in accordance with the 2010 analysis, the jet p_T thresholds are scaled only for the first two H_T bins and remain fixed for all subsequent bins. The thresholds are listed in Table 1.

In 2010, a cut-and-count approach was used, in which an extrapolation from a low-H_T control region ($250 < H_T < 350$ GeV) into the H_T signal region ($H_T > 350$ GeV) was performed in order

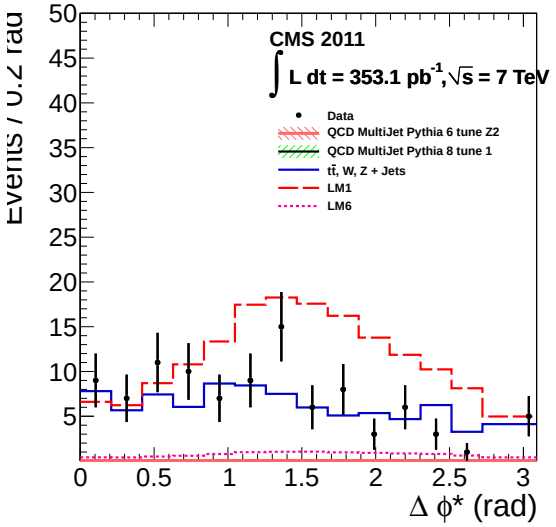

(a) $\Delta\Phi^*$ after α_T shows flat behaviour as expected from standard model processes.

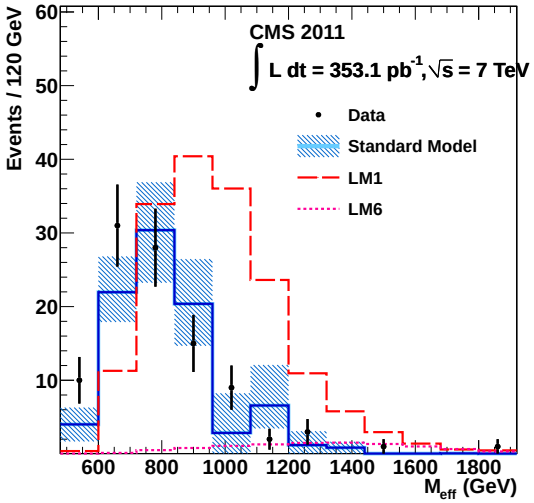

(b) The Effective mass of the events passing α_T shows agreement with standard model, electro-weak processes.

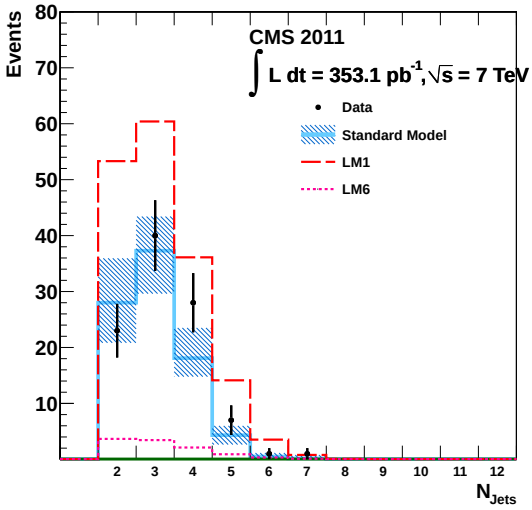

(c) Shows the jet multiplicity after the α_T selection cut. A high level of agreement is observed between the simulated standard model distribution and that measured in Data

Figure 2: Comparisons between Data and Monte Carlo after the α_T selection cut.

to estimate the SM background. The analysis now makes use of the full range $H_T > 275\,\text{GeV}$ (without a control region) and tests observed yields in the all-hadronic channel against SUSY models using muon and photon control samples, to predict the EWK background components, and various constraints which include the following two assumptions: zero QCD contamination throughout the entire H_T region-of-interest; and constant R_{α_T} as a function of H_T for the remaining EWK backgrounds. The details of this approach are discussed in Sec. 6.

Figure 3 (left) shows the evolution of R_{α_T} versus H_T, as measured in data collected during 2011 and also obtained from MC simulations of SM, SM+LM1 and SM+LM6. The data (SM

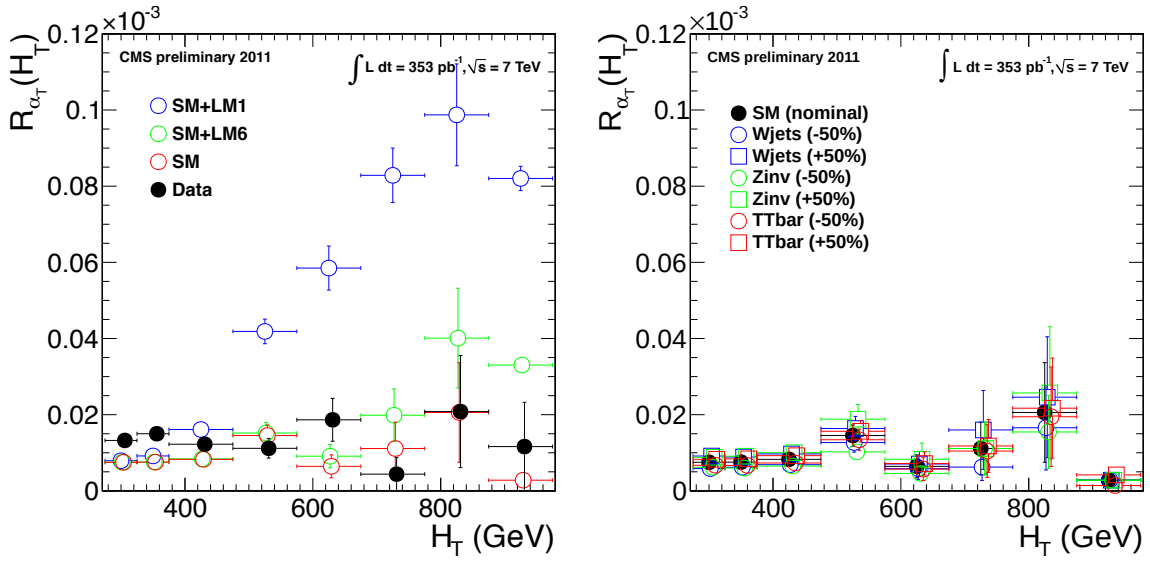

Figure 3: (Left) The dependence of R_{α_T} on H_T for events with Njet $\geq$2. (Right) Dependence of R_{α_T} on H_T when varying the effective cross-section of the three major EWK background components individually by $\pm$50%. (Markers are artificially offset for clarity.)

expectations) are consistent with the flat hypothesis, with χ^2/dof= 7.9/6 (7.8/6) and p-values of 0.24 (0.24). The SM+LM1 and SM+LM6 are not consistent with the flat hypothesis.

Figure 3 (right) demonstrates the independence of R_{α_T} on H_T, based on MC simulations even when varying the effective cross-section of the three major EWK background components individually by as much as $\pm$50%. In each case, the behaviour is always consistent with the flat hypothesis, with a p-value of at least 0.18. This is how the assumption of flat behaviour is tested against the systematic uncertainties associated with the cross-section measurements of the different EWK backgrounds.

4.3 Estimation of background from $t\bar{t}$ and W + jets events using a muon control sample

A data-driven estimate of the backgrounds from unidentified leptons or hadronic tau decays originating from high-p_T W bosons is obtained through the definition of a muon control sample. In this sample we explicitly select W's decaying to a muon and a neutrino in the phase-space of the signal. This is performed in the same H_T bins as for the hadronic signal selection.

All cuts on jet-based quantities are consistent with those in the cut flow in the search region. For Muon identification and kinematic cuts we use recommendations of the $t\bar{t}$ group. The muons selected have $p_T > 20$ GeV and $|\eta| < 2.1$. In order to select W events we have the following additional cuts:

- $M_T > 30$ GeV, where M_T is the transverse mass of the W candidate.
- Δ R(jet,muon) > 0.5
- MHT/HT > 0.4, a cut on p_T(W)
- No second global muon (using loose muon definition used to veto in hadronic cut-flow). This reduces $Z \rightarrow \mu\mu$.

The number of events from W+jet events in the hadronic selection W^{had}_{data} can be estimated from the event yield in the muon sample, W^{-}_{data}. This is done using the expected relative ratio of

those two types of events. The value of this ratio is extracted from the Monte Carlo, and thus the estimated number of W events in the hadronic analysis is calculated by

$$W^{had}_{data} = W^{\mu}_{data} \times \frac{W^{had}_{MC}}{W^{\mu}_{MC}}.$$

In the lowest two H_T bins, the value of $\frac{W^{had}_{MC}}{W^{\mu}_{MC}}$ is extracted separately. However, due to low Monte Carlo statistics in the highest H_T bins, one value for the ratio is used for $H_T > 375$ GeV. This MC translation factor shows little dependenc on H_T (see Table 2).

Table 2 shows the split of the muon control sample numbers and corresponding background prediction in the different H_T bins. Errors quoted on predictions correspond to statistical errors and an additional conservative systematic uncertainty of 30%, as used in the previous analysis [5]. We observe a good agreement between data and MC, as shown both before (Figure 4) and after (Figure 5) the α_T cut.

Table 2: Muon sample predictions with 353pb^{-1}. Errors quoted on predictions correspond to statistical errors and an additional conservative systematic uncertainty of 30%, as used in the previous analysis.

H_T Bin (GeV)	275–325	325–375	375–475	475–575
MC W + $t\bar{t}$	126.2	47.8	30.6	11.3
MC μ+ jets	121.8	46.3	31.9	10.4
MC Ratio	1.04	1.03	0.97	0.97
Data μ+ jets	111.5	41.1	34.2	12.7
W + $t\bar{t}$ Prediction	115.6 $\pm 10.8_{stat}$ $\pm 34.7_{syst}$	42.4 $\pm 6.5_{stat}$ $\pm 12.7_{syst}$	33.2 $\pm 5.6_{stat}$ $\pm 10.0_{syst}$	12.3 $\pm 3.4_{stat}$ $\pm 3.7_{syst}$
H_T Bin (GeV)	575–675	675–775	775–875	875–∞
MC W + $t\bar{t}$	1.9	1.8	0.9	0.2
MC μ+ jets	3.6	2.1	0.1	0.1
MC Ratio	0.97	0.97	0.97	0.97
Data μ+ jets	5.9	1.0	0.0	0.0
W + $t\bar{t}$ Prediction	5.7 $\pm 2.3_{stat}$ $\pm 1.7_{syst}$	0.9 $\pm 1.3_{stat}$ $\pm 0.3_{syst}$	0.0 $\pm 1.1_{stat}$	0.0 $\pm 1.1_{stat}$

4.3.1 Estimation of background from Z $\rightarrow \nu\bar{\nu}$+ jets from photon + jets events

Z $\rightarrow \nu\bar{\nu}$ +jet events form an irreducible background. An estimate of this background can be obtained from the γ + jets process, which has a larger cross section but kinematic properties similar to those of Z $\rightarrow \nu\bar{\nu}$ events when the photon is ignored [3]. The γ + jet sample is selected by requiring photons, i.e. localized electromagnetic depositions satisfying tight isolation criteria [11], with p_T greater than 100 GeV, $|\eta|$ less than 1.45 and $\Delta R(\gamma, \text{jet}) > 1$. Ignoring the photon, the same hadronic final state selection as in the signal selection is applied.

Table 3 shows the observed counts in the photon control sample and the corresponding background predictions.

5 Systematic uncertainties on signal efficiency

The systematic uncertainties on the signal efficiency will be evaluated in coordination with the other hadronic SUSY analyses.

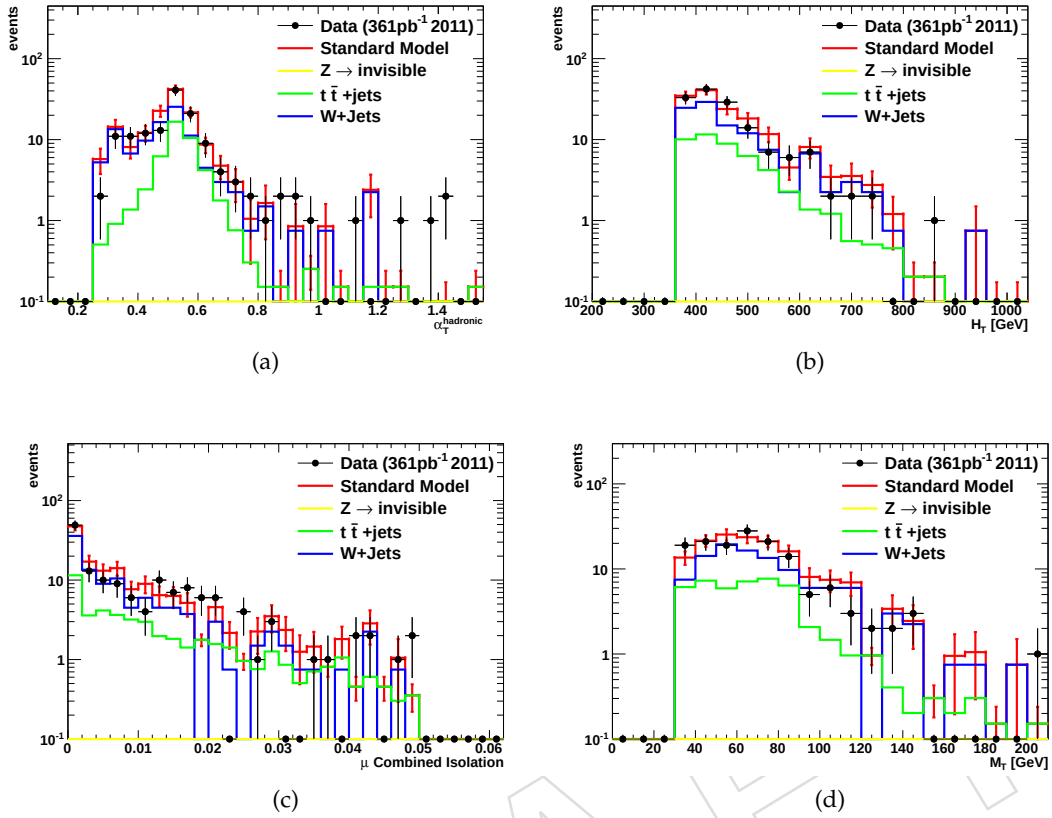

Figure 4: Data - Monte Carlo comparisons for the Muon Control Selection before the $\alpha_T > 0.55$ cut is applied, shown for (a) α_T, (b) H_T, (c) Muon Combined Isolation and (d) M_T. A cut of HT >375 GeV has been applied, to select the region of fixed jet thresholds. Data corresponds to 361pb$_{-1}$ of 2011 CMS data at 7TeV.

Table 3: Photon Sample Predictions 353pb^{-1}

H_T Bin (GeV)	275–325	325–375	375–475	475–575
MC Z $\to \nu\bar{\nu}$	67.8	30.9	20.3	15.1
MC γ+ jets	218.4	84.3	54.2	17.3
MC Ratio	0.31	0.37	0.47	0.47
Data γ+ jets	302.7	112.2	63.3	25.6
Z $\to \nu\bar{\nu}$ Prediction	93.9 $\pm 4.7_{stat}$ $\pm 37.6_{syst}$	41.1 $\pm 3.4_{stat}$ $\pm 16.4_{syst}$	29.6 $\pm 3.2_{stat}$ $\pm 11.8_{syst}$	12.0 $\pm 2.1_{stat}$ $\pm 4.8_{syst}$
H_T Bin (GeV)	575–675	675–775	775–875	875–∞
MC Z $\to \nu\bar{\nu}$	2.3	0.0	0.7	0.0
MC γ+ jets	8.3	0.7	0.9	0.7
MC Ratio	0.47	0.47	0.47	0.47
Data γ+ jets	9.0	3.8	2.3	0.8
Z $\to \nu\bar{\nu}$ Prediction	4.2 $\pm 1.2_{stat}$ $\pm 1.7_{syst}$	1.8 $\pm 0.8_{stat}$ $\pm 0.7_{syst}$	1.1 $\pm 0.6_{stat}$ $\pm 0.4_{syst}$	0.4 $\pm 0.5_{stat}$ $\pm 0.1_{syst}$

6 Framework for Statistical Interpretation

This section outlines the statistical framework used for the limit interpretation of the observed yields of the H_T shape analysis.

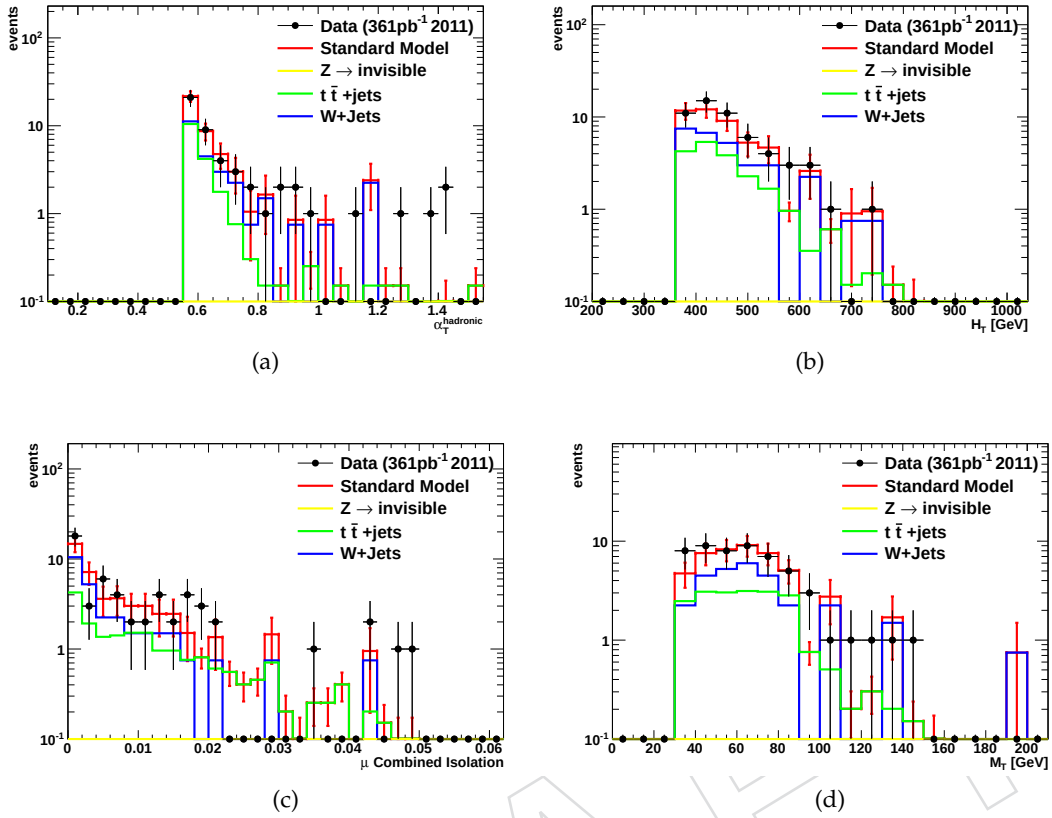

(a) (b)

(c) (d)

Figure 5: Data - Monte Carlo comparisons for the Muon Control selection after the $\alpha_T > 0.55$ cut is applied, shown for (a) α_T, (b) H_T, (c) Muon Combined Isolation and (c) M_T. A cut of HT >375 GeV has been applied, to select the region of fixed jet thresholds. Data corresponds to 361pb$_{-1}$ of 2011 CMS data at 7TeV.

6.1 Hadronic Selection

Let N be the number of H_T bins. The bins need not have equal width. Let n^i represent the number of events observed with $\alpha_T > 0.55$ in each H_T bin i. Then we write the likelihood of the observations this way:

$$L_{hadronic} = \prod_i \text{Pois}(n^i | b^i + s^i) \quad (1)$$

where b^i represents the expected Standard Model background in bin i, and s^i represents the expected number of signal events in bin i.

6.2 Background Models

We assume that $b^i \equiv EWK^i + QCD^i$, where EWK^i is the expected yield of electroweak events in bin i, and QCD^i is the expected yield of QCD events in bin i.

6.2.1 QCD

We model QCD^i as described in Section 6.6, i.e. $QCD^i(A_{QCD}, k_{QCD})$. One can assume either:

- R_{QCD} is constant or falling ($k_{QCD} \geq 0$)

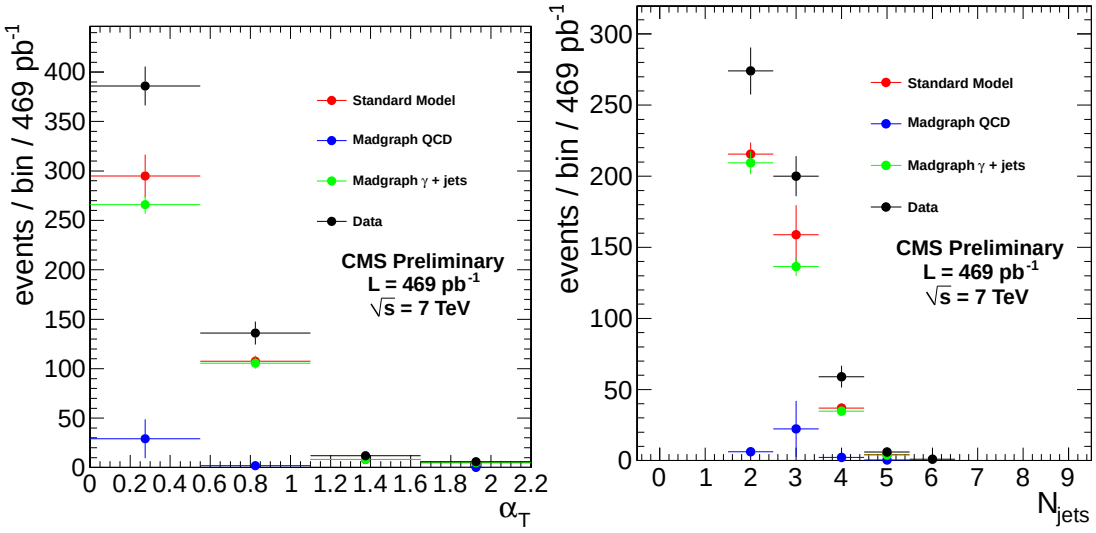

(a) (b)

Figure 6: Data-Monte Carlo comparisons for the photon control sample. $H_T > 375$ GeV and $\not{H}_T / H_T > 0.4$ are required. Left: the distribution of α_T. Right: the distribution of the number of jets.

- Zero QCD ($A_{QCD} = 0$)

6.2.2 EWK

We define $Z^i_{inv} \equiv f^i_{Zinv} \times EWK^i$, and $ttW^i \equiv (1 - f^i_{Zinv}) \times EWK^i$. The variables Z^i_{inv} and ttW^i are used in Section 6.5. Each f^i_{Zinv} is a fit parameter, and is limited to be between zero and one. One can either allow EWK^i to float, or assume one of these:

- R_{EWK} has the functional form described in Section 6.6, i.e. $EWK^i(A_{EWK}, k_{EWK})$
- R_{EWK} is constant or falling ($k_{EWK} \geq 0$)
- R_{EWK} is constant ($k_{EWK} = 0$)

6.3 Testing the Goodness-of-Fit of the SM-only Hypothesis

In Equation 1, we set $s^i = 0$ for all i. We determine the set of parameter values which maximizes the likelihood function using one of the methods discussed in Section 6.6.2, and note the corresponding value L^{data}_{max} of the likelihood. The likelihood function (using these parameter values) is then used as a p.d.f. for the observations to generate many pseudo-experiments. For each pseudo-experiment, we maximize the likelihood function over all parameters, and note the corresponding value L_{max}. We create a histogram of L_{max}, find the quantile of L^{data}_{max}, and quote the result as a p-value.

6.4 Testing Particular SUSY Models

Let x represent the cross-section for the model in question, and let l represent the recorded luminsosity. Let ϵ^i_{had} be the analysis efficiency as simulated for the model in H_T bin i. We take the uncertainty on efficiency to be fully correlated among the bins. Let δ represent the relative uncertainty on the signal yield in a bin i. Let ρ_{sig} represent the "correction factor" to the signal yield which accommodates systematic uncertainties. Let f be the parameter of interest, for which we shall determine the allowed interval. We write the likelihood of the observations this

way:

$$L_{hadronic} = \text{Gaus}(1.0|\,\rho_{sig}, \delta) \times \prod_i \text{Pois}(n^i|\,b^i + f\rho_{sig} x l \epsilon^i_{had}) \tag{2}$$

If the upper limit of the interval for f is less than one, then we consider the model incompatible with the data.

6.5 Electroweak Background Constraints

In each bin of H_T, we have two measurements: n_{ph}, and n_{mu}, representing the event counts in the photon and muon control samples. Each of these measurements has a corresponding Monte Carlo expectation: MC_{ph}, and MC_{mu}. The Monte Carlo also gives expected amounts of Z_{inv} and $t\bar{t}+W$ in the hadronically-selected sample: $MC_{Z_{inv}}$ and $MC_{t\bar{t}+W}$. Let i label the H_T bin, let σ^{inp}_{phZ} and σ^{inp}_{muW} represent the relative systematic uncertainties for the control sample constraints. Define

$$r^i_{ph} = \frac{MC^i_{ph}}{MC^i_{Z_{inv}}};\; r^i_{mu} = \frac{MC^i_{mu}}{MC^i_{t\bar{t}+W}} \tag{3}$$

We treat the systematics as fully correlated among the H_T bins. We use this likelihood:

$$L_{ph} = \text{Gaus}(1.0|\,\rho_{phZ}, \sigma^{inp}_{phZ}) \times \prod_i \text{Pois}(n^i_{ph}|\,\rho_{phZ} r^i_{ph} Z^i_{inv}) \tag{4}$$

$$L_{mu} = \text{Gaus}(1.0|\,\rho_{muW}, \sigma^{inp}_{muW}) \times \prod_i \text{Pois}(n^i_{mu}|\,\rho_{muW} r^i_{mu} ttW^i + s^i_{mu}) \tag{5}$$

The parameters ρ_{phZ} and ρ_{muW} represent "correction factors" which accommodate systematic uncertainty. The variable Z^i_{inv} represents the expected number of $Z \to \nu\bar{\nu}$ events in H_T bin i of the hadronically selected sample. The variable ttW^i represents the expected number of events from SM W-boson production (including top quark decays) in H_T bin i of the hadronically selected sample.

We define $s^i_{mu} \equiv f\rho_{sig} x l \epsilon^i_{mu}$, where ϵ^i_{mu} is the analysis efficiency of the muon-selection on the SUSY model in question in H_T bin i, and the other parameters are defined in Section 6.4.

6.6 H_T Evolution Method

The hypothesis that the α_T ratio falls exponentially in H_T can be written this way:

$$R_{\alpha_T}(H_T) = Ae^{-kH_T} \tag{6}$$

where A and k are parameters whose values will be determined. A constant ratio is equivalent to requiring $k = 0$. Let m_i represent the number of events observed with $\alpha_T \leq 0.55$ in each H_T bin i.

The expected background is written thus:

$$b_i = \int_{x_i}^{x_{i+1}} \frac{\mathrm{d}N}{\mathrm{d}H_T}(x) A e^{-kx}\,\mathrm{d}x. \tag{7}$$

where $\frac{\mathrm{d}N}{\mathrm{d}H_T}$ is the distribution of H_T for events with $\alpha_T \leq 0.55$, x_i is the lower edge of the bin, and x_{i+1} is the upper edge of the bin (∞ for the final bin).

6.6.1 Delta-function H_T distribution

Assume

$$\frac{\mathrm{d}N}{\mathrm{d}H_T}(x) = m_i \delta(x - \langle H_T \rangle_i), \tag{8}$$

i.e. within a bin the whole distribution occurs at the mean value of H_T in that bin. Then

$$b_i = \int_{x_i}^{x_{i+1}} m_i \delta(x - \langle H_T \rangle_i) A e^{-kx} \, \mathrm{d}x = m_i A e^{-k\langle H_T \rangle_i}. \tag{9}$$

6.6.2 Likelihood Model

The likelihood function used is the product of the likelihood functions described in the previous sections:

$$L = L_{hadronic} \times L_{mu} \times L_{ph} \tag{10}$$

If one lets EWK^i float (i.e., does not assume a functional form for R_{EWK}), then there are $5 + 2N$ nuisance parameters: A_{QCD}, k_{QCD}, $\{EWK^i\}$, $\{f_Z inv^i\}$, as well as the "systematic" variables ρ_{phZ}, ρ_{muW}, ρ_{sig}. If one assumes an exponential form for R_{EWK}, then there are $7 + N$ nuisance parameters: remove $\{EWK^i\}$ from the above set, and include A_{EWK} and k_{EWK}.

7 Final Results

In this section we discuss the results of the statistical interpretation of the H_T dependent yield measurements in the all-hadronic, W+jet, and Photon+Jet samples. The H_T distributions shown in Figure 7, 8, and 9 are the result of the simultaneous fit to the H_T dependent yield in the all-hadronic, W+jet and photon+jet sample, respectively. A good agreement between the measured H_T distributions and the best fit is observed in all three distributions, indicating that the number of events found in data is compatible with the SM background expectation predicted by the fit. The results of the fit are tabulated in Table 4.

The hypothesis of constant R_{α_T} with respect to H_T is well reproduced by the best fit (see Figure 10). With a p-value of 0.6 for the SM-only hypothesis no significant deviation is observed.

We interpret this lack of signal as a limit on the allowed parameter space of the CMSSM. Figure 11 shows the 95% exclusion limit in the m_0-$m_{1/2}$ plane for $\tan\beta = 10$ and $A_0 = 0\,\mathrm{GeV}$ calculated with a two-sided profilelikelihood method. At low values of m_0 the limit is cut off at $m_0 = 450\,\mathrm{GeV}$ where the signal scan ends. Squark and gluino masses of 1 TeV can be excluded for values of the common scalar mass at the GUT scale $m_0 < 420\,\mathrm{GeV}$.

8 Summary

In this note we have presented a search for supersymmetry in dijet and multijet events using the α_T variable. The analysis presents an update of the published paper [1] with some further refinements. The study is currently based on an integrated luminosity of $350\,\mathrm{pb}^{-1}$, corresponding to a factor 10 increase in analysed data compared to the 2010 analysis. The observed H_T distribution for events with $\alpha_\mathrm{T} > 0.55$ is in good agreement with the SM expectation obtained from data control samples. In the absence of a signal, limits on the allowed parameter space in the CMSSM were set which exceed those set by previous analyses.

Table 4: Fit Results 353pb^{-1}

H_T Bin (GeV)	275–325	325–375	375–475	475–575
W + $t\bar{t}$ background	165.5	64.9	43.9	12.3
$Z \rightarrow \nu\bar{\nu}$ background	91.1	40.3	28.2	10.5
Total Background	256.6	105.2	72.1	22.8
Data	254.0	118.0	66.0	19.0
H_T Bin (GeV)	575–675	675–775	775–875	875–∞
W + $t\bar{t}$ background	4.5	1.3	0.3	0.7
$Z \rightarrow \nu\bar{\nu}$ background	3.4	1.7	1.0	0.5
Total Background	7.9	3.0	1.3	1.1
Data	11.0	1.0	2.0	1.0

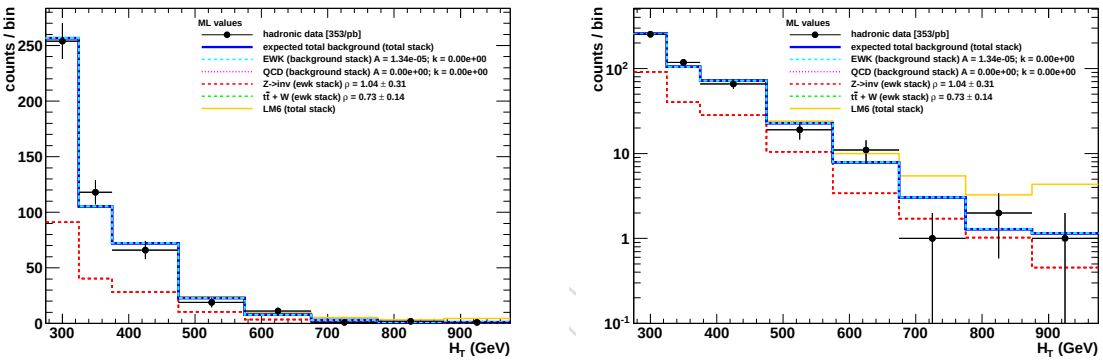

Figure 7: H_T distribution for events in the hadronic signal sample with linear (left) and logarithmic y-scale (right). Shown are the events observed in data (black points), the outcome of the fit (blue line) and a breakdown of the individual background contributions as predicted by the control samples. A possible signal contribution from benchmark point LM6 is indicated as well (yellow line).

References

[1] CMS Collaboration Collaboration, "Search for Supersymmetry in pp Collisions at 7 TeV in Events with Jets and Missing Transverse Energy", *Phys.Lett.* **B698** (2011) 196–218, arXiv:1101.1628. * Temporary entry *. doi:10.1016/j.physletb.2011.03.021.

[2] CMS Physics Analysis Summary, CMS PAS SUS-09-001.

[3] CMS Physics Analysis Summary, CMS PAS SUS-08-005.

[4] L. Randall and D. Tucker-Smith, "Dijet Searches for Supersymmetry at the LHC", *Phys.Rev.Lett.* **101 221803** (2008).

[5] CMS Analysis Note, CMS-AN 2010/242.

[6] M. Cacciari, G. P. Salam, and G. Soyez, "The anti-kt jet clustering algorithm", *JHEP* **0804:063** (2008).

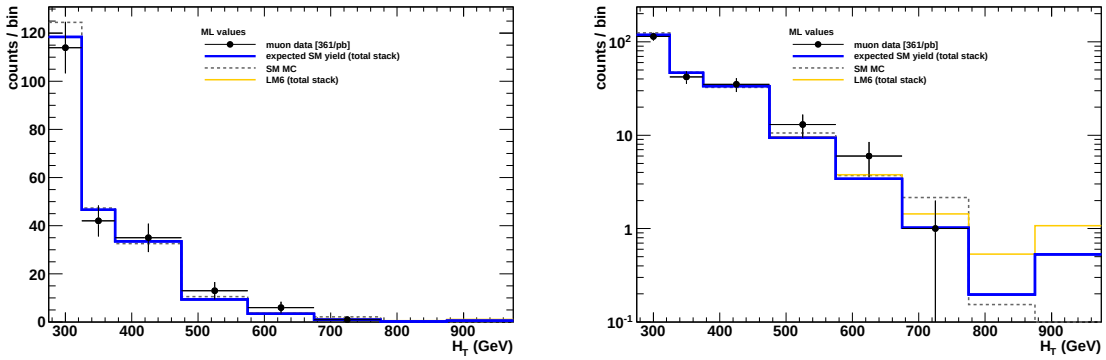

Figure 8: H_T distribution for events selected in the muon control sample with linear (left) and logarithmic y-scale (right). Shown are the events observed in data (black points), the outcome of the fit (blue line) and the MC expectation (dashed line). A possible signal contribution from benchmark point LM6 is indicated as well (yellow line).

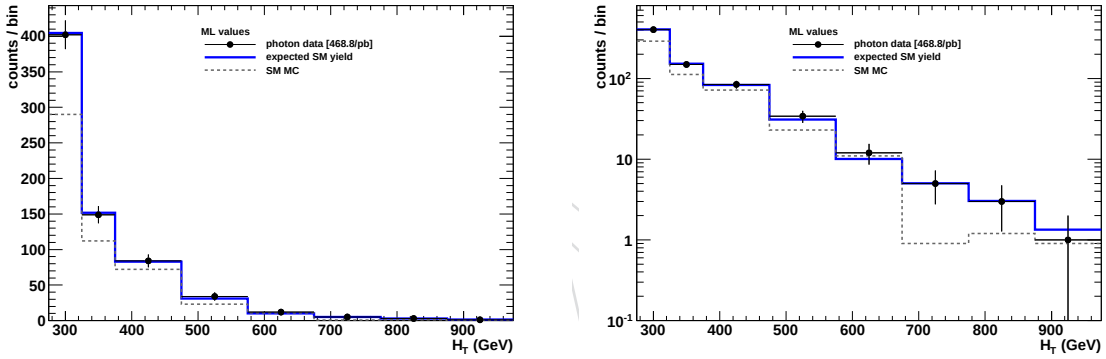

Figure 9: H_T distribution for events selected in the photon control sample with linear (left) and logarithmic y-scale (right). Shown are the events observed in data (black points), the outcome of the fit (blue line) and the MC expectation (dashed line).

[7] CMS Collaboration, "Calorimeter Jet Quality Criteria for the First CMS Collision Data", *CMS Physics Analysis Summary* **JME-09-008** (2009).

[8] CMS Collaboration, "Electron reconstruction and identification at $\sqrt{s} = 7$ TeV", *CMS Physics Analysis Summary* **EGM-10-004** (2010).

[9] CMS Collaboration, "Performance of muon identification in pp collisions at $\sqrt{s} = 7$ TeV", *CMS Physics Analysis Summary* **MUO-10-002** (2010).

[10] CMS Collaboration, "Photon reconstruction and identification at $\sqrt{s} = 7$ TeV", *CMS Physics Analysis Summary* **EGM-10-005** (2010).

[11] See: https://twiki.cern.ch/twiki/bin/view/CMS/PhotonID.

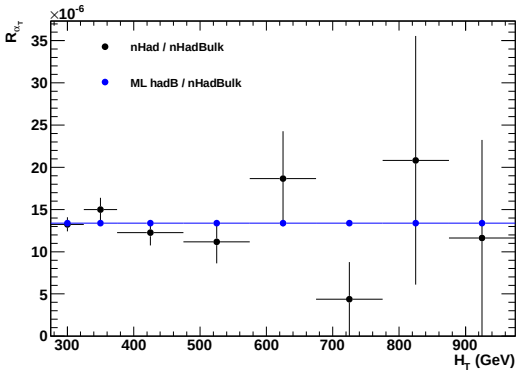

Figure 10: R_{α_T} as a function of H_T as observed in data (black points) and the result of the fit assuming constant behaviour (blue line).

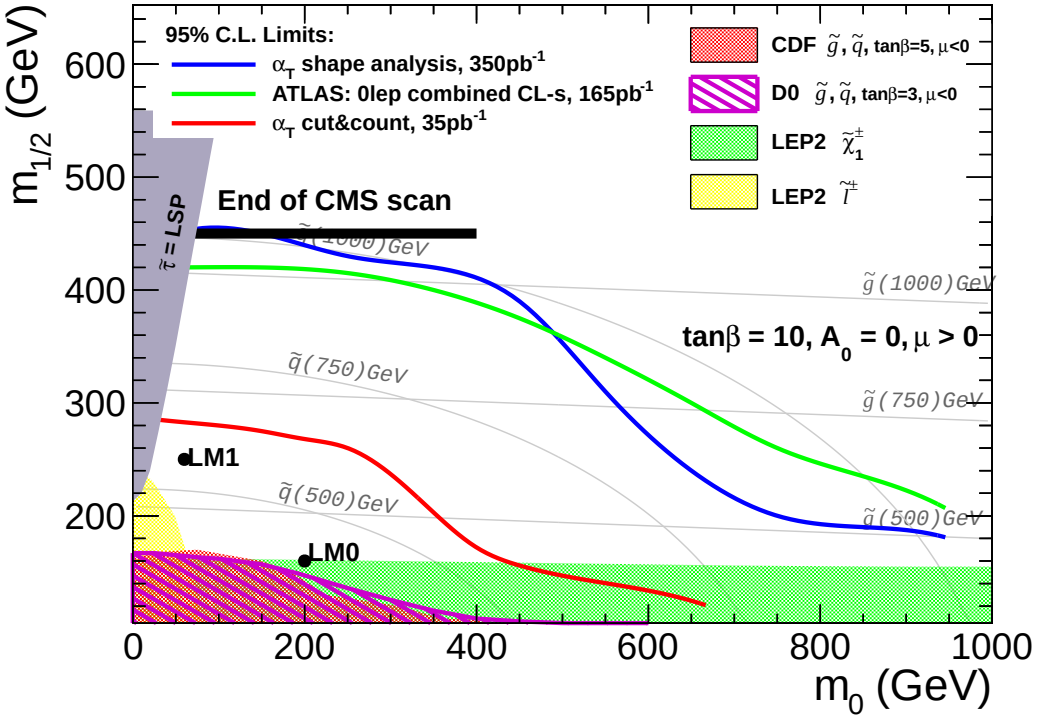

Figure 11: 95% exclusion limit in the $m_0 - m_{1/2}$ plane of the CMSSM (LO cross sections).